Full-Wave Design and Realization of Multicoupled Dual-Mode Circular Waveguide Filters

José R. Montejo-Garai and Juan Zapata, *Member, IEEE*

***Abstract*—A new full-wave method for the design and realization of dual-mode circular waveguide filters is presented. The rigorous CAD is a combination of the mode-matching and the finite-element techniques, which permits obtaining the Generalized Scattering Matrix for all the blocks that compose the structure (rectangular slots, cross-irises, and screws). The finite thickness of the irises, the higher order mode interaction, as well as the coupling and tuning screws are rigorously taken into account. A systematic design process for the different elements will be described. A full prediction of resonant out-of-band spurious is accomplished prior to the filter construction. Special attention is devoted to the circuital model in order to save a great deal of computational effort in the final adjustment. A four-pole elliptic circular waveguide cavity filter has been designed and constructed. The experimental filter results show excellent agreement with theory.**

I. Introduction

THE GROWING demand for available channels in satellite communication systems during the last decades has led to the design of microwave filters having sophisticated transfer functions. The necessity of providing small guard band, linear phase, as well as high selectivity between adjacent channels has forced introduction of finite transmission zeros. This makes it possible to improve the out-of-band amplitude characteristic in contrast to the pure Chebyshev or Butterworth (all-pole) response or to obtain self-equalized responses. Furthermore, the reduction of scarce resources on a spacecraft, like weight and volume has been a constant over the years. All the previously considered requirements are performed by the dual-mode structure.

As is well-known, a cavity can support an infinite number of electromagnetic field configurations or modes. Based on this idea, Ragan [1] suggested the possibility of building a circular waveguide filter with two degenerate modes. Lin [2] extended the above design using five degenerate modes. In 1970, Williams [3] designed the first longitudinal multimode four-order elliptic filter with two dual-mode cavities. From the seventies onward, a great effort was dedicated to the development of the theory and feasibility of the dual-mode filters [4]–[6]. Later on, asymmetric realization [7] and triple mode configuration were carried out.

However, in spite of the progress made in multimode filters during the last years, some design troubles have not been solved yet. For example, to obtain the coupling value of slots and cross-irises between cavities, it is necessary to resort to approximate models. Bethes' theory of diffraction by small holes along with Cohn's polarizability measurement diagrams are presently employed [9]. Nevertheless, an important number of corrections have been introduced over the initial models in order to improve them [10]–[12]:

1) the first correction factor concerns the influence of the iris resonance effect on the coupling;
2) the second one takes into account the finite iris thickness; and
3) the third one considers the variations of the incident electromagnetic fields within the aperture region.

Additionally, a closed-form formula has been recently derived for the normalized susceptance of a general aperture discontinuity in the transverse plane of a circular waveguide as a function of the aperture polarizability [13].

Although the above considerations have improved the calculation of the coupling coefficients, the experience indicates that their accuracy is not sufficient. For this reason, different sized slots and cross-irises have to be built prior to the final prototype. In addition, the coupling between the degenerate modes in the same cavity provided by the screw inserted at a 45° angle has never been considered. The same occurs with tuning screws. Consequently, despite the improvement of approximated methods, the final design and adjustment of dual-mode filters are, even in our days, really prolix tasks. The manufacturing is also an extremely expensive process.

The aim of this paper is to present a new rigorous systematic design procedure for circular waveguide dual-mode filters. As a consequence of this process, the manufacturing cost is lowered, and the final adjustment and tuning time is also reduced. The procedure is a combination of full-wave methods and circuital models. This mixture joins the power of full-wave techniques and the information provided by simplified circuits. As a result, an efficiency CAD has been developed.

II. Full-Wave Method

The proposed full-wave technique is a combination of the mode-matching and the finite-element techniques (MM-FEM) [14]. The waveguide structure under study can be considered as the connection of two kinds of blocks. The first block [Fig. 1(a)] is composed of two arbitrarily shaped waveguide sections linked through an arbitrarily shaped iris. This generic sketch represents the coupling arising between waveguides in dual-mode filters. In the case of dual-mode circular waveguide filters (DMCWF's), this sketch is particularized for

Manuscript received August 8, 1994; revised November 10, 1994. This work was supported in part by Alcatel Espacio S.A.

The authors are with the Grupo de Electromagnetismo Aplicado y Microondas, Departamento de Electromagnetismo y Teoría de Circuitos, Universidad Politécnica de Madrid, E.T.S.I. Telecomunicación, Ciudad Universitaria S/N, 28040 Madrid, Spain.

IEEE Log Number 9410702.

two situations. For the input and output couplings, the input waveguide is rectangular, and the output one is circular. For intercavity coupling, both waveguides are circular. The second block [Fig. 1(b)] is a circular waveguide length with three screws inside. The screw tilted 45° couples the two degenerate modes, while the other two screws are tuning each mode independently. Therefore, applying the combined MM-FEM to the elements mentioned above, their Generalized Scattering Matrixes (GSM's) are obtained. These GSM's rigorously take into account the finite thicknesses of the irises and the screws and the higher order mode interactions. Accordingly, any n-order DMCWF can be considered as a cascade of the previously described blocks.

For the derivation of the GSM's, every block is divided into simple discontinuities between waveguides of different cross-sections. At both sides of the discontinuity, the electromagnetic field can be expressed as

$$\begin{aligned}
\vec{E}_t^{\,t} &= \sum_{i=1}^{\infty} [a_i e^{-\gamma_i^{\mathrm{I}} z} + b_i e^{\gamma_i^{\mathrm{I}} z}]\vec{e}_i^{\,\mathrm{I}} \\
\vec{H}_t^{\mathrm{I}} &= \sum_{i=1}^{\infty} [a_i e^{-\gamma_i^{\mathrm{I}} z} - b_i e^{\gamma_i^{\mathrm{I}} z}]\vec{h}_i^{\mathrm{I}} \\
\vec{E}_t^{\mathrm{II}} &= \sum_{j=1}^{\infty} [a_j e^{\gamma_j^{\mathrm{II}} z} + b_j e^{-\gamma_j^{\mathrm{II}} z}]\vec{e}_j^{\,\mathrm{II}} \\
\vec{H}_t^{\mathrm{II}} &= \sum_{j=1}^{\infty} [-a_j e^{\gamma_j^{\mathrm{II}} z} + b_j e^{-\gamma_j^{\mathrm{II}} z}]\vec{h}_j^{\mathrm{II}}
\end{aligned} \tag{1}$$

$a_i^{\mathrm{I}}, b_i^{\mathrm{I}}, a_j^{\mathrm{II}}, b_j^{\mathrm{II}}$ are the unknown complex amplitudes of the forward and backward waves in z direction at both sides of the discontinuity. $\gamma_i^{\mathrm{I}}, \gamma_j^{\mathrm{II}}$ are the propagation constants. $\vec{e}_i^{\,\mathrm{I}}, \vec{h}_i^{\mathrm{I}}, \vec{e}_j^{\,\mathrm{II}}, \vec{h}_j^{\mathrm{II}}$ are the transverse electrical and magnetic components in each side of the discontinuity. If the cross-sections of the waveguides are rectangular or circular in shape, the transverse electromagnetic components have analytical expressions as Fourier-Fourier and Fourier-Bessel expansions, respectively. On the contrary, if the waveguide modes have no analytical expressions, numerical methods must be considered to obtain the complete mode set. In such cases, the Finite Element Method (FEM) has been employed to solve Helmholtz's equation. The reason for using FEM is its flexibility concerning the geometry. Matching the tangential electrical and magnetic field components (1), the GSM of a simple discontinuity is obtained

$$\begin{bmatrix} b^{\mathrm{I}} \\ b^{\mathrm{II}} \end{bmatrix} = \begin{bmatrix} [S_{11}] & [S_{12}] \\ [S_{21}] & [S_{22}] \end{bmatrix} \begin{bmatrix} a^{\mathrm{I}} \\ a^{\mathrm{II}} \end{bmatrix}. \tag{2}$$

Although the screws have circular cross-sections, an equivalent square cross-section has been used [15] [Fig. 1(b)]. Thus, the dual-mode structure can be considered as several transverse discontinuities linked by homogeneous waveguide lengths leading to a two-dimensional problem (GSM's computation) followed by a one-dimensional problem (the link of the GSM's).

When the variational principle of Helmholtz's equation is employed to solve any arbitrarily shaped homogeneous waveguide, the finite element formulation can be scalar [16].

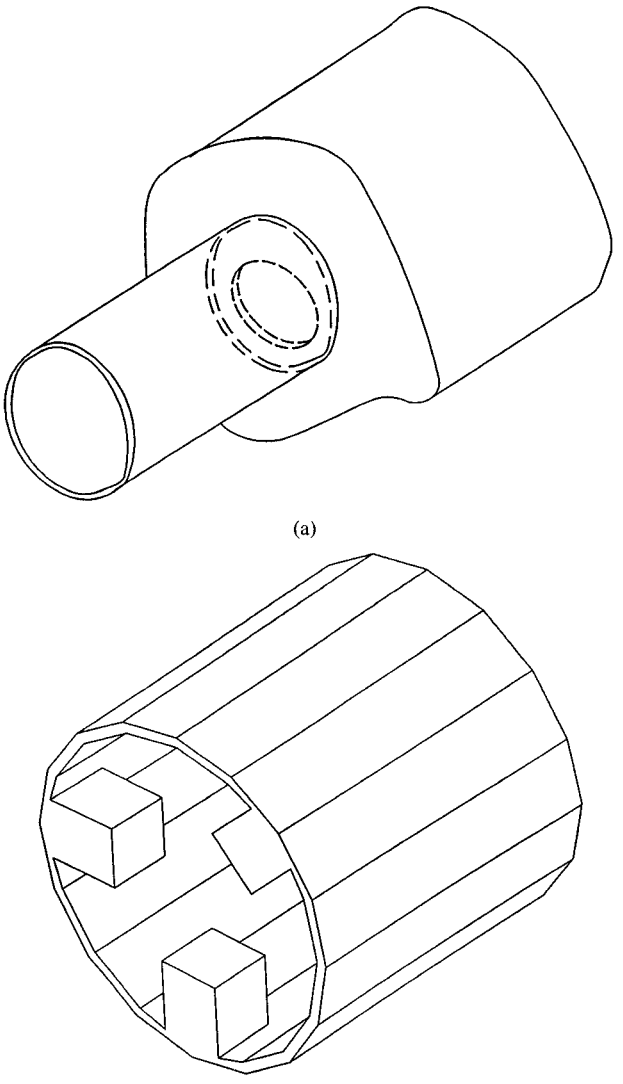

(a) (b)

Fig. 1. (a) General block for iris coupling between waveguides in dual-mode filters. (b) Circular-circular-triseptum discontinuity.

It has been broadly verified that this formulation is spurious free and that the convergence is very good even if the structure presents edges. Since the scalar element only gives the axial field component, E_z for TM and H_z for TE modes, the transverse components are calculated from the axial ones there where the error is minimum [17]. A very important point in order to develop a CAD is to determine automatically the FEM mesh from the geometric input data. For example, in the case of the triseptum circular waveguide (coupling and tuning screws), the mesh is generated by defining only the radii of both the circular waveguide and the screws and the depth of these. When a change is made in any geometric datum, the mesh is automatically regenerated and the GSM recalculated.

The method of analysis described above has been validated by studying some simple circuits that include the elemental DMCWF's blocks. For irises whose area is very small compared to the area of the circular waveguide, artificial intermediate discontinuities of zero length have been introduced. As a result of this, the number of employed modes is reduced, and numerical instabilities are avoided [18]. The first analyzed

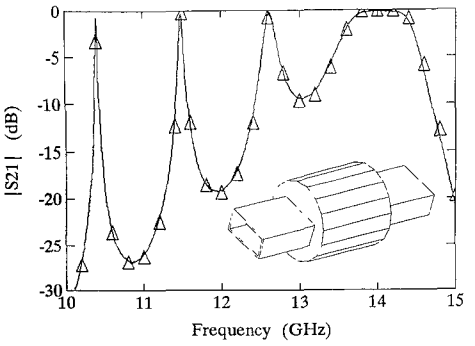

Fig. 2. Circular cavity filter response, input and output waveguide WR75 (19.05 mm × 9.525 mm), coupling slots (9.7 mm × 3 mm × 1 mm), cavity length 100 mm, radius 12 mm. (△ △ △ △) measured; (——) simulated.

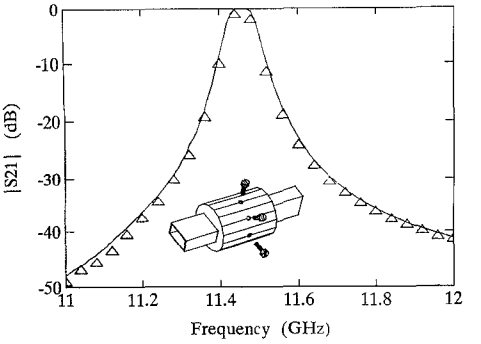

Fig. 3. Two-pole circular waveguide filter response, input and output rectangular waveguide WR75 (19.05 mm × 9.525 mm), coupling slots (9.7 mm × 3 mm × 1 mm), cavity length 50 mm, radius 12 mm, vertical screw = 1.74 mm, horizontal screw = 1.64 mm, coupling screw = 2.72 mm. (△ △ △ △) measured; (——) simulated.

circuit is a circular cavity resonator shown in Fig. 2 that includes the input and output slots of a DMCWF. Due to the symmetries of the structure, only TE_{mn} and TM_{mn} modes with vertical perfect magnetic conductor wall and horizontal perfect electric conductor wall symmetry were considered in the analysis. Fig. 2 shows the comparison between measured and computed data. An excellent agreement is observed.

A similar technique has been employed to analyze the cross-iris coupling between circular waveguide cavities. In this case, several rectangular waveguides are used as intermediate artificial steps between the cross-iris and the circular waveguide. In the final artificial step between the cross-iris and its circumscribed rectangular waveguide, the mode ratio is chosen as close as possible to the area ratio between them. This method was applied to analyze circuits like those shown in [19], [20]. This rule of thumb, which is essential for CAD, has been extensively verified by measurements. Finally, the discontinuity between circular triseptum and circular sections shows a very good convergence due to the fact that the area ratio is approximately one to one. This consideration is pointed out by the excellent agreement between measurements and theoretical results. Fig. 3 represents the measurement and computed response of a two-pole circular waveguide filter with three screws inside. The modes are selected using the criteria established in [21]. Once the different blocks have been investigated and their convergence behavior controlled, the process of systematic design for DMCWF's will be explained.

III. Design Method

So far, the design of DMCWF's have been based on theoretical curves and expensive trial and error tests. The new full-wave systematic design avoids these drawbacks applying the efficiency of MM and the flexibility of FEM. Although the first synthesis technique was developed by Atia and Williams [5], the powerful procedure proposed by Rhodes [22] has been employed. This makes use of the double cross-coupled network. Since admittance inverter coupling unity reactances are equivalent to the mutual coupling, the canonical structure of Atia and Williams is no more than the cross-coupled network of Rhodes. To obtain the in-line configuration, the canonical structure must be appropriately processed [23]. Fig. 4 represents the double cross-coupled network of a four-

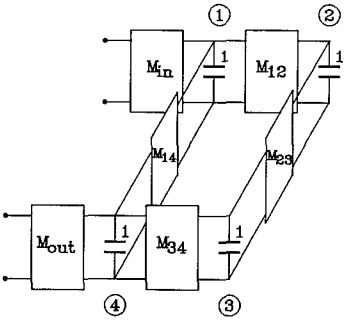

Fig. 4. Double cross-coupled network prototype $N = 4$.

pole filter for which the canonical and in-line structures are the same. It will serve as an example without loss of generality when extended to higher orders.

The circuit model input and output admittance couplings $M_{\text{in}}, M_{\text{out}}$ are easily identified with the rectangular-slot-circular waveguide block. M_{12} and M_{34} are the coupling screws. M_{23} is the vertical arm of the cross-iris, and M_{14} is the cross-coupling, i.e., the horizontal arm. The steps followed to obtain all geometric dimensions are given below.

A. Theoretical Synthesis of the Filter

Using a synthesis method, the coupling matrix is attained. Then, every normalized coefficient of this matrix is identified with its corresponding physical coupling, i.e., input-output slots, cross-iris arms, and coupling screws of the filter.

B. Calculation of the Initial Sizes of the Input and Output Slots

It is convenient to increase slightly the typical thickness of the slots because in this way their sensitivity to the mechanical tolerance is reduced, and the final weight of the filter is not appreciably increased. For a given coupling value, the width and length of the slots will be larger because the thickness is also larger. As a consequence, the mechanization process is eased, and since the sensitivity is reduced, the adjustment process is simplified. The thickness and width of the slots are fixed, and the length is computed in order to obtain the coupling value. With this strategy, it is necessary to adjust only one parameter.

To calculate the initial length of the slots, the S_{22} parameter of the fundamental mode in the circular waveguide, extracted

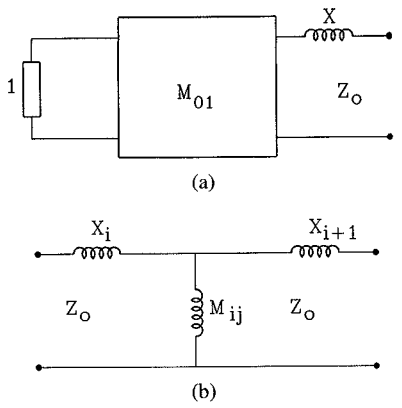

Fig. 5. (a) Equivalent monomode lumped circuit for rectangular-slot-circular waveguide structure. (b) Equivalent monomode lumped circuit for circular-cross-iris-circular waveguide structure.

from the GSM of the rectangular-slot-circular waveguide block, is related to the coupling value $M_{01} = M_{\text{in}} = M_{\text{out}}$ by means of an equivalent monomode circuital model (Fig. 5(a)). The equivalence between the lumped constant circuit and the microwave circuit is established by applying the equality of the reactance slope parameter of both circuits [9]. From this equivalence, the following expressions are deduced:

$$M_{01} = \frac{1 - |S_{22}|^2}{1 + |S_{22}|^2 - 2\,\text{Re}[S_{22}]} Z_0$$
$$X = \frac{2\,\text{Im}[S_{22}]}{1 + |S_{22}|^2 - 2\,\text{Re}[S_{22}]} Z_0$$
$$Z_0 = \frac{2}{n\pi}\left(\frac{\lambda_0}{\lambda_{g0}}\right)^2 \tag{3}$$

where Re[] is the real part, Im[] is the imaginary part, λ_{go} is the guide wavelength at the center frequency, λ_o is the free space wavelength, n is the number of $\lambda/2$ sections, and X is the reactance due to the aperture in the cavity. As the S_{22} parameter depends on the length of the slots, (3) allows the relation of both the coupling and the length.

C. Calculation of the Initial Dimensions of the Cross-Iris Arms

The above considerations, concerning the thickness and width of the slots, are also applied to the cross-iris. To calculate the initial length of the horizontal arm, the S_{11} and S_{12} parameters of the fundamental mode in the circular waveguide, extracted from the GSM of the circular-cross-iris-circular waveguide block, are related to its corresponding cross coupling value $M_{ij}(M_{14}, M_{45}, \cdots)$ of the coupling matrix by means of an equivalent monomode circuital model (Fig. 5(b)). The equality of the reactance slope parameter has been again applied, giving

$$M_{ij} = \frac{-1}{\text{Im}\left[\dfrac{1 - S_{11}}{S_{12}}\right]} Z_0$$
$$X_i = \left[\text{Re}\left[\frac{1 - S_{11}}{S_{12}}\right] - 1\right] M_{ij}$$
$$Z_0 = \frac{2}{n\pi}\left(\frac{\lambda_0}{\lambda_{go}}\right)^2 \tag{4}$$

where X_i is the reactance related to the aperture. The length of the vertical arm is initially taken as the same as the horizontal arm. Once the length of the horizontal arm has been calculated, the cross-iris is rotated 90°, and using the same procedure, the new length of the vertical arm is obtained with $M_{ij}(M_{23}, M_{36}, \cdots)$. It has been extensively verified that the fact of considering the cross-iris as two independent perpendicular slots leads to inaccurate design lengths. The reason lies in the four singular points belonging to the cross-iris section, which perturb the electromagnetic field configuration.

D. First Adjustment of the Iris Dimensions and the Cavity Length

Generally, the radius of the cavity is determined by spurious mode separation. Therefore, only the cavity length is a design parameter. The iris apertures produce a foreshortening effect upon cavity length that must be taken into account. From the equivalent monomode circuits, an initial value for the size of the irises has been obtained. A full-wave simulation of the filter response without coupling and tuning screws allows the modification of the size of the input and output slots and the horizontal arms (vertical polarization) as well as cavity length. The curve of reference to verify it is the theoretical response of the double cross-coupled network, in which the admittance inverters representing coupling screws have been eliminated ($M_{i,i+1} i = 1, 3, \cdots n - 1$). Comparing both responses, the circuital and the full-wave, the sizes are adjusted. By rotating 90 degrees the cross-irises inside the cavities, the same process is followed to correct the vertical arms. At the end of this step, all the iris sizes and the cavity lengths are adjusted. When the screws are inserted in the final step, new higher order mode interactions will appear and will force the recalculation of the iris sizes.

E. Calculation of the Initial Depths of the Coupling and Tuning Screws

The next step calculates the initial depths of the screws inserted inside the cavity. Although there are two different cases, the coupling screw and the tuning screw, both are solved in a similar way. Considering a piece of circular waveguide, short-circuited in both sides, whose length was calculated in the previous step, a screw is introduced for tuning vertical or horizontal polarization. The natural frequencies of this configuration can be obtained by solving the equation [24], [25]

$$\det[S + I] = 0 \tag{6}$$

where S is the GSM of the structure of Fig. 6, and I is the unit matrix. The lower natural frequency corresponds to the resonant frequency affected by the screw. Changing the depth of the screw inside the cavity, a curve representing frequency-variation versus depth is drawn. Since the length of the cavity was corrected (step d) to amend the vertical polarization TE_{113} resonant frequency, only the horizontal tuning screw is inserted to tune the horizontal polarization TE_{113}. Thus, a good estimation of the initial depth of the horizontal tuning screw is obtained. A similar procedure is used for the screw tilted 45° (the coupling screw). From the two resonant frequencies corresponding to the insertion of a perfect electric and magnetic conductor wall (Fig. 6), the

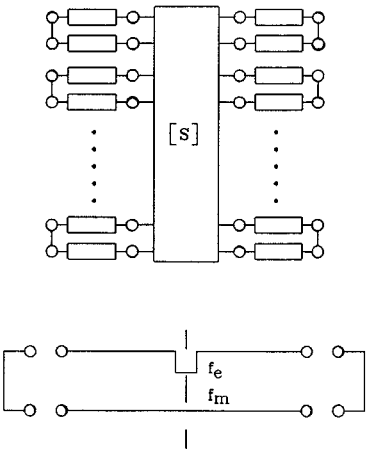

Fig. 6. Multimode network for calculating the coupling provided by the screw inserted at a 45° angle and the resonant frequency variation due to the horizontal tuning screw.

coupling coefficient $M_{ij}(M_{12}, M_{34}, \cdots)$ is calculated [22]

$$M_{ij} = \frac{f_e^2 - f_m^2}{f_e^2 + f_m^2}. \tag{7}$$

A curve showing the relation between the coupling and the depth of the screw is obtained. Thus, by means of this step, the initial depths of the coupling and the horizontal tuning screws are obtained. These dimensions will serve as very good starting points in the final iterative adjustment.

It must be noted that the calculation of the depths is repeated for every different cavity, i.e, when the irises that load it are also different.

F. Tuning and Final Adjustment

The introduction of the screws inside the cavities leads to the recalculation of the previous dimensions because new higher order mode interactions appear. However, since the initial values are close to the definitive ones, a small number of iterations are required. The adjustment is simplified if the equivalent double cross-couple network is utilized. The process is as follows: once a full-wave response of the initial filter is calculated, its corresponding coupling matrix along with every resonant frequency are deduced from the lumped equivalent circuit. By comparing both results, the differences between the actual and the theoretical coupling values and the deviations of the resonant frequencies can be found. As said before, the tuning adjustment is only accomplished on the horizontal polarization because, once the filter verifies the isolation, matching, and bandwidth requirements, its center frequency is shifted by shortening or prolonging all the cavities. Therefore, only one tuning screw per cavity is employed.

The aim of employing the equivalent lumped circuit is to know how the different coupling and tuning values affect the response in order to change their corresponding dimensions in the full-wave simulation. To sum up, a smart optimization by means of the perfect knowledge of the filter operation is achieved. This kind of optimization of iris and screw dimensions reduces dramatically the computational time. Finally, a full-wave simulation of the filter is obtained prior to its physical realization.

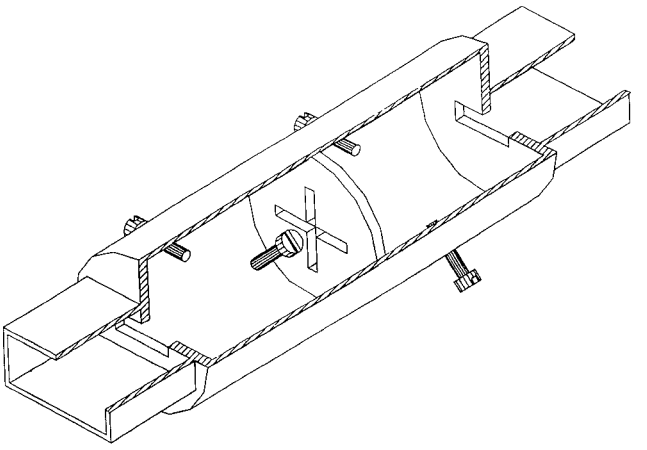

Fig. 7. Configuration of the designed four-pole dual-mode circular waveguide filter. Only one tuning screw per cavity is employed.

IV. Results

The verification of the design method expounded above has been accomplished by constructing a four-pole elliptic DMCWF.

The desired electrical characteristics of the filter are

Center frequency	11.8 Ghz
Bandwidth	100 Mhz
Minimum return losses	≥20 dB
Out of band rejection	≥15 dB

Fig. 7 represents the designed filter configuration. It is formed by two circular cavities connected by two identical slots to the input and output rectangular waveguides. Also, a cross-iris connects both cavities. The coupling between the two degenerate modes in each cavity is realized by the coupling screw and, as explained before, the design only needs the horizontal tuning screw. For this band and considering the resonant mode T_{113}, the diameter of the waveguide is chosen to obtain the out-of-band spurious as far as possible. Therefore, the previously fixed values are

Diameter of the cavities	28.0 mm
Thickness of all irises	1.5 mm
Width of the slots	3.0 mm
Width of the both arms of the cross-iris	2.0 mm
Diameter of the screws	2.0 mm

The dimensions to calculate are

Length of the cavities	L_C
Length of the slots (M_{01} coupling)	L_S
Length of the horizontal arm (M_{14} coupling)	L_H
Length of the vertical arm (M_{23} coupling)	L_V
Depth of the coupling screws (M_{12} coupling)	D_C
Depth of the horizontal tuning screw	D_T

By means of the proposed method, the following values are calculated:

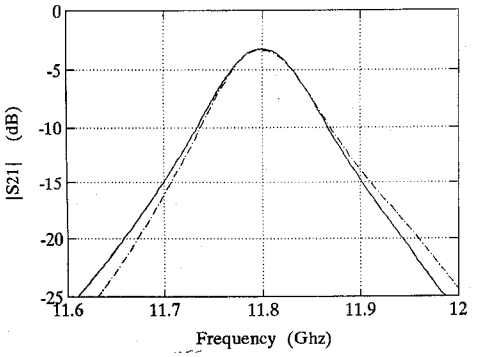

Fig. 8. Response of the lumped equivalent circuit of the four-pole filter in Fig. 7 when the couplings provided by the screws are eliminated (——). Full-wave simulation of the filter without screws (— · — · —).

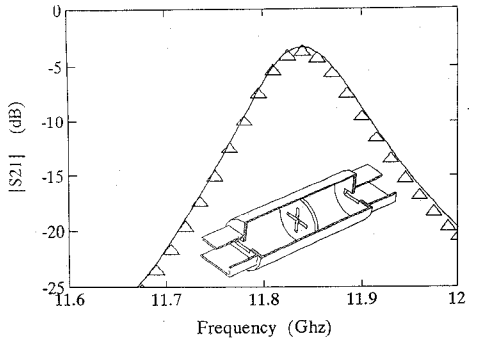

Fig. 9. Response of the dual-mode filter without screws. (△ △ △△) measured; (——) full-wave simulated. Dimensions: cavity length 43.87 mm, radius 12 mm, iris thicknesses 1.5 mm, slot lengths 10.05 mm, slot widths 3.0 mm, arm widths 2.0 mm, horizontal arm length 7.65 mm, vertical arm length 8.75 mm.

Step a) The normalized coupling matrix is

$$M = \begin{bmatrix} 0 & 0.80382 & 0 & -0.42705 \\ 0.80382 & 0 & 0.86843 & 0 \\ 0 & 0.86843 & 0 & 0.80382 \\ -0.42705 & 0 & 0.80382 & 0 \end{bmatrix}$$
$$M_{01} = 1.03487 \tag{8}$$

Step b) Applying (3), the initial length of the slots is $L_S = 9.975$ mm.

Step c) Applying (4), the initial length of the horizontal arm is $L_H = 7.56$ mm, and the initial length of the vertical arm is $L_V = 8.74$ mm.

Step d) Fig. 8 represents the comparison between the response of the lumped equivalent circuit when the coupling screws ($M_{12} = M_{34}$) are eliminated and the full-wave simulation after the initial lengths of the slots and the horizontal arm have been corrected. If M_{14} is substituted by M_{23} in the circuit model, and the cross-iris is rotated 90° in the full-wave simulation, a similar comparison to that in Fig. 8 leads to the recalculation of the length of the vertical arm. Additionally, a new cavity length is calculated when adjusting the horizontal arm length. Fig. 9 shows the comparison between the full-wave simulation and the measurement when this correction is accomplished. The final results of this step are $L_C = 44.0$ mm, $L_S = 10.01$ mm, $L_H = 7.62$ mm, and $L_V = 8.80$ mm.

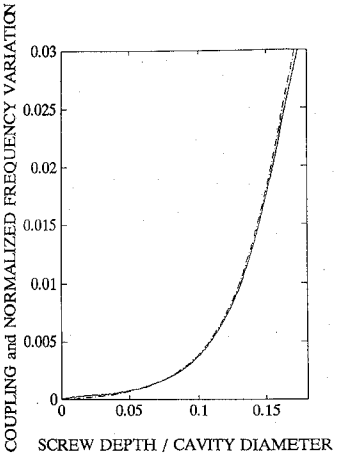

Fig. 10. Curve for the calculation of the initial depths of the coupling (——) and horizontal tuning screws (— · — · —).

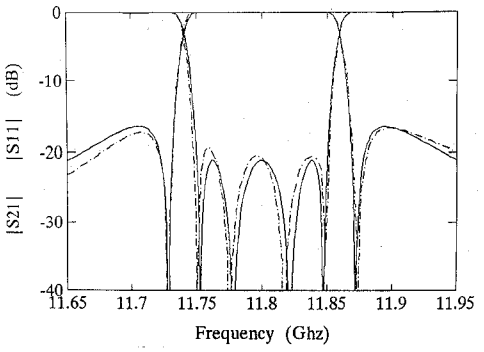

Fig. 11. Comparison between the theoretical response (——) of the filter obtained in the synthesis process and the full-wave simulation (— · — · —) after optimization procedure.

Step e) Fig. 10 shows the relation between the coupling value and the depth of the coupling screw considering the length of the cavity computed in the previous step. From this curve, an initial depth for the coupling screw is deduced, $D_C = 3.30$ mm. In addition, Fig. 10 shows the relation between the variation of the resonant frequency of the circular cavity ($L_C = 44.0$ mm) and the depth of the horizontal tuning screw. From this curve is deduced, $D_T = 4.16$ mm. The mutual interaction between the tuning and the coupling screws is minimized by the position in which they are placed in each cavity (Fig. 7).

Step f) The geometrical dimensions previously calculated are very close to the final ones and are taken as starting points in a smart optimization process. First, a full-wave simulation is performed, then the equivalent circuit parameters are modified to fit the full-wave response. In this way, the dimensions that must be changed are found, and the process is repeated. Since the equivalent lumped circuits cannot take into account all the interactions, the last adjustment is carried out by resorting to the full-wave simulation only. After a few optimization steps, the full-wave response verifies the filter characteristics, and the process is terminated. Fig. 11 shows the comparison between the full-wave simulation and the theoretical response of the

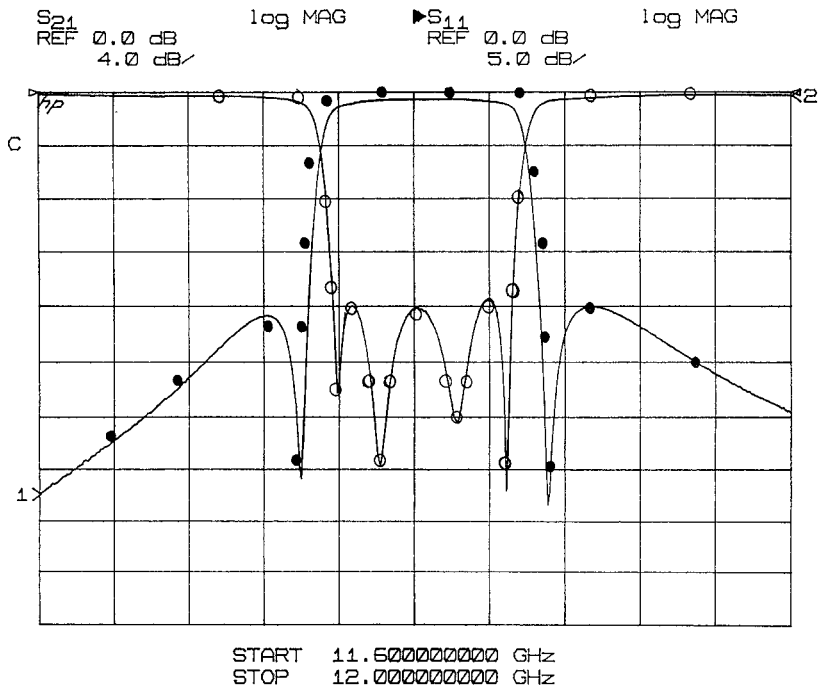

Fig. 12. (——) Measured response of the constructed four-pole elliptic filter, (• • • •) S_{21} parameter full-wave simulation, and (o o oo) S_{11} parameter full-wave simulation.

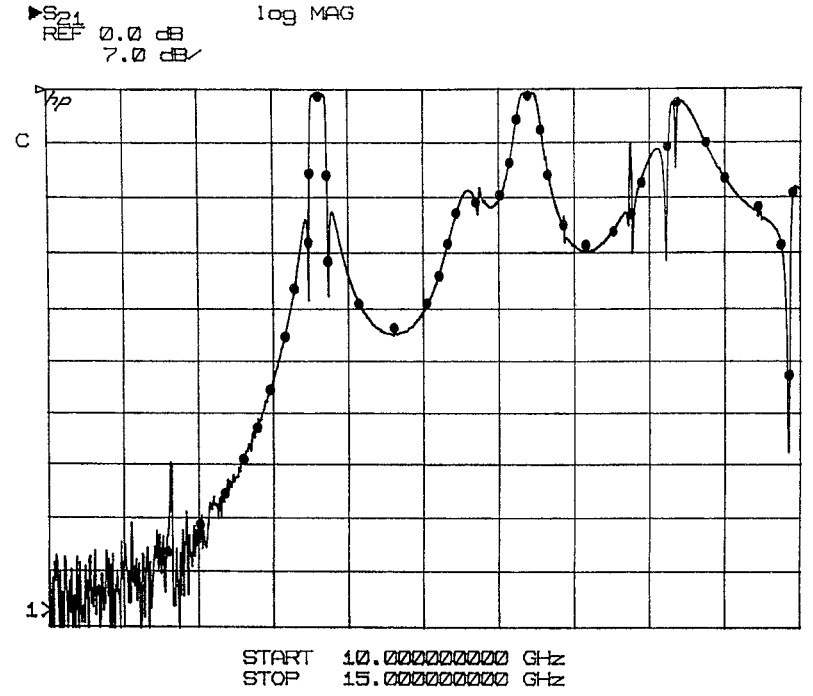

Fig. 13. (——) Measured far out-of-band rejection of the constructed four-pole elliptic filter; (• • • •) full-wave simulation.

circuit model. The final dimensions are

Length of the cavities	$L_C = 43.87$ mm
Length of the slots	$L_S = 10.05$ mm
Length of the horizontal arm	$L_H = 7.65$ mm
Length of the vertical arm	$L_V = 8.75$ mm
Depth of the coupling screws	$D_C = 3.57$ mm
Depth of the horizontal tuning screws	$D_T = 3.82$ mm

The designed filter was constructed on brass. The tuning process in the laboratory was a very fast task as a consequence of the exact computation of the iris dimensions and the reduction of the number of tuning screws. Fig. 12 represents the comparison between the measurement and the full-wave simulation in its operational band. The agreement is excellent. Fig. 13 shows the comparison between the wide-band measurement and the full wave simulation. All the different

spurious are predicted in their positions and levels. Again, the agreement between both results is excellent. A whole simulation of the filter (Fig. 12) with 25 frequency points consumes about 2 CPU hours in a HP series 9000 model 730.

V. Conclusion

A new full-wave method for designing DMCWF's, which is based on the combined MM-FEM, has been presented. Since the method includes the finite iris thickness and the screws inside the cavity, the higher mode interaction is rigorously taken into account. A step-by-step design process, which gives the initial iris dimensions and the depths of the screws has been explained. The final adjustment is accomplished by interaction with the circuital model, making possible a smart optimization. The advances of this method are: 1) The out-of-band response obtained leads to a full prediction of resonant spurious prior to the filter construction. 2) The final adjustment is simplified because only two screws per cavity are required, and their initial positions are known. 3) There is no adjustment of the iris dimensions, therefore the cost is dramatically lowered. A four-pole elliptic filter has been designed, and the full-wave prediction shows excellent agreement with the measurements.

References

[1] G. L. Ragan, "Microwave transmission circuits," in *Radiat. Lab. Series MIT.* New York: McGraw-Hill, 1948, vol. 9, pp. 673–677.

[2] W. G. Lin, "Microwave filters employing a single cavity excited in more than one mode," *J. Appl. Phys.*, vol. 22, pp. 989–1001, 1965.

[3] A. E. Williams, "A four-cavity elliptic waveguide filter," *IEEE Trans. Microwave Theory Tech.*, vol. MTT-20, pp. 258–265, Apr. 1972.

[4] A. E. Atia and A. E. Williams, "New types of waveguide bandpass filters for satellite transponders," *Comsat Tech. Rev.*, vol. 1, no. 1, pp. 21–43, Fall 1971.

[5] A. E. Atia, A. E. Williams, and R. W. Newcomb, "Narrow-band multiple-coupled cavity synthesis," *IEEE Trans. Circuits Syst.* vol. CAS-21, no. 5, pp. 649–655, Sept. 1974.

[6] A. E. Atia and A. E. Williams, "Dual-mode canonical waveguide filter," *IEEE Trans. Microwave Theory Tech.*, vol. MTT-25, pp. 1021–1026, Dec. 1977.

[7] R. J. Cameron and J. D. Rhodes, "Asymmetric realization for dual-mode bandpass filters," *IEEE Trans. Microwave Theory Tech.*, vol. MTT-29, pp. 51–58, Jan. 1981.

[8] W. C. Tang and S. K. Chaudhuri, "A true elliptic-function filter using triple-mode degenerate cavities," *IEEE Trans. Microwave Theory Tech.*, vol. MTT-32, no. 11, pp. 1449–1454, Nov. 1984.

[9] G. Matthaei, L. Young, and E. M. T. Jones, *Microwave Filters, Impedance-Matching Networks, and Coupling Structures.* New York: McGraw-Hill, 1964, pp. 229–243.

[10] S. B. Cohn, "Microwave coupling by large apertures," *Proc. IRE.*, vol. 7, pp. 696–699, June 1952.

[11] R. Levy, "Improved single and multiaperture waveguide coupling theory, including explanation of mutual interactions," *IEEE Trans. Microwave Theory Tech.*, vol. MTT-28, pp. 331–338, Apr. 1980.

[12] A. Jennings and R. L. Gray, "Extension of Levy's large-aperture design formulas to the design of circular irises in coupled-resonator waveguide filters," *IEEE Trans. Microwave Theory Tech.*, vol. MTT-32, pp. 1489–1493, Nov. 1984.

[13] G. B. Easthanm and K. Chang, "Analysis and closed-form solutions of circular and rectangular apertures in the transverse plane of a circular waveguide," *IEEE Trans. Microwave Theory Tech.*, vol. 39, pp. 718–723, Apr. 1991.

[14] J. Zapata and J. García, "Analysis of passive microwave structures by a combined finite element-generalized scattering matrix method," in *Proc. 1991 N. Amer. Radio Sci. Meet.*, Ontario, Canada, June 1991, p. 146.

[15] J. M. Garai and J. Zapata, "Rigorous analysis of posts in rectangular and circular waveguides," in *Abstracts URSI Meet.*, Ann Arbor, MI, June 28–July 2, 1993.

[16] P. Silvester, "A general high-order finite element waveguide analysis program," *IEEE Trans. Microwave Theory Tech.*, vol. MTT-17, pp. 204–210, Apr. 1969.

[17] J. E. Akin, *Application and Implementation of Finite Elements Methods.* Academic, 1982.

[18] U. Papziner and F. Arndt, "Field theoretical computer-aided design of rectangular and circular iris coupled rectangular or circular waveguides cavity filters," *IEEE Trans. Microwave Theory Tech.*, vol. 41, pp. 462–471, Mar. 1993.

[19] J. Zapata *et al.*, "Field-theory analysis of cross-iris coupling in circular waveguide resonator," *Microwave Opt. Technol. Lett.*, vol. 6, no. 16, pp. 905–907, Dec. 1993.

[20] J. Zapata *et al.*, "Design of coupling and tuning devices for dual-modes microwave filters in circular waveguides," in *Progr. in Electromagnetic Res. Symp.*, JPL CALTECH, Pasadena, CA, July 12–16, 1993.

[21] J. Montejo-Garai *et al.*, "Full wave analysis of tuning and coupling post in dual-mode circular waveguides filters," *Microwave Opt. Technol. Lett.*, pp. 505–507, Aug. 1994.

[22] J. D. Rhodes, "A low-pass prototype network for microwave linear phase," *IEEE Trans. Microwave Theory Tech.*, vol. 18, pp. 290–301, June 1980.

[23] J. D. Rhodes and I. H. Zabalawi, "Synthesis of symmetrical dual mode in-line prototype networks," *Circuit Theory and Applications*, vol. 8, pp. 145–160, 1980.

[24] H. C. Chang, K. A. Zaki, and A. E. Atia, "Evanescent-mode coupling of dual-mode rectangular waveguide filters," *IEEE Trans. Microwave Theory Tech.*, vol. 39, pp. 1307–1312, Aug. 1991.

[25] X. P. Liang, K. A. Zaki, and A. E. Atia, "Dual mode coupling by square corner cut in resonators and filters," *IEEE Trans. Microwave Theory Tech.*, vol. 40, pp. 2294–2302, Dec. 1992.

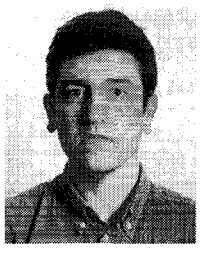

José R. Montejo-Garai was born in Vitoria-Gasteiz, Spain, in 1965. He received the Ingeniero de Telecomunicación degree from the Universidad Politécnica de Madrid, Madrid, Spain, in 1990.

Since 1990 he has been Profesor Titular de Escuela Universitaria interino at the Departamento de Electromagnetismo y Teoría de Circuitos of the Universidad Politécnica de Madrid where he is working towards his Ph.D. degree. His research interests include the analysis and characterization of waveguide structures using numerical methods, specially finite elements, and CAD for microwave and millimeter-wave passive devices.

Juan Zapata (M'93) received the Ingeniero de Telecomunicación degree in 1970 and the Ph.D. degree in 1974, both from the Universidad Politécnica de Madrid, Madrid, Spain.

Since 1970 he has been with the Grupo de Electromagnetismo Aplicado y Microondas at the Universidad Politécnica de Madrid where he became an assistant professor in 1970, associate professor in 1975, and professor in 1983. His current research interests include interactions of electromagnetic fields with biological tissues, computer aided design for microwave passive circuits, and numerical methods in electromagnetism.